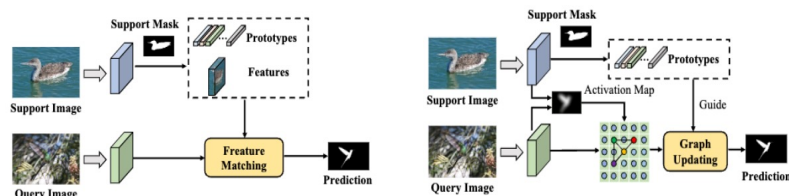


Motivation



(a). Existing few-shot segmentation methods generate support prototypes/features from the support image, then implement feature matching to obtain mask prediction for the query image. However, merely leveraging support information usually fail to work when support and query image exhibits large appearance/scale variance.

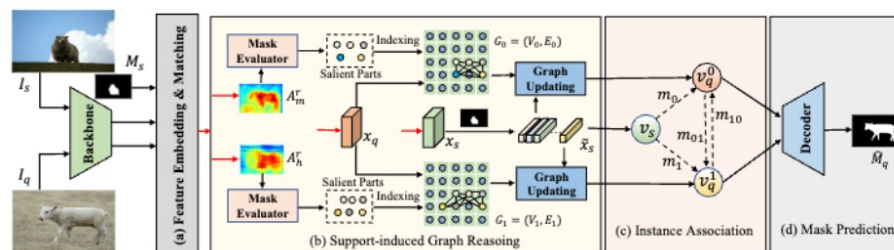
(b). Our main idea is to explicitly enrich the query context information with the guidance of support information. In practice, we adopt a support-induced graph convolutional network to achieve this goal.

Contribution

(a) We propose a support-induced graph convolution network (SiGCN), which utilizes the proposed IA and SiGR modules to capture complementary context from the query and the support set, for addressing the appearance variation problem in the FSS task.

(b) We propose a novel graph updating mechanism, in which support prototypes guide the node updating in the query graphs. This mechanism brings a significant performance gain to the proposed SiGCN.

Methodology



(a) A support-induced graph reasoning module to mine context information from query image.

(b) An instance association module to explore information from both support and query images.

Experiment Results

		Results on PASCAL5 ¹											
Methods	Backbone	1-shot					5-shot						
		Fold-0	Fold-1	Fold-2	Fold-3	Mean	FB-IoU	Fold-0	Fold-1	Fold-2	Fold-3	Mean	FB-IoU
OSLSM (BMVC'17) [21]	VGG16	33.6	55.3	40.9	33.5	40.8	61.3	35.9	58.1	42.7	39.1	43.9	61.5
co-FCN (ICLRW'18) [18]	VGG16	36.7	50.6	44.9	32.4	41.1	60.1	37.5	50.0	44.1	33.9	41.4	60.2
PFENet (TPAMI'20) [24]	VGG16	56.9	68.2	54.4	52.4	58.0	72.0	59.0	69.1	54.8	52.9	59.0	72.3
HSNet (ICCV'21) [15]	VGG16	59.6	65.7	59.6	54.0	59.7	73.4	64.9	69.0	64.1	58.6	64.1	76.6
PFENet (TPAMI'20) [24]	ResNet50	61.7	69.5	55.4	56.3	60.8	73.3	63.1	70.7	55.8	57.9	61.9	73.9
RePRI (CVPR'21) [11]	ResNet50	59.8	68.3	62.1	48.5	59.7	-	64.6	71.4	71.1	59.3	66.6	-
SAGNN (CVPR'21) [27]	ResNet50	64.7	69.6	57.0	57.3	62.1	73.2	64.9	70.0	57.0	59.3	62.8	73.3
MMNet (ICCV'21) [26]	ResNet50	62.7	70.2	57.3	57.0	61.8	-	62.2	71.5	57.5	62.4	63.4	-
HSNet (ICCV'21) [15]	ResNet50	64.3	70.7	60.3	60.5	64.0	76.7	70.3	73.2	67.4	67.1	69.5	80.6
CyCTR (NIPS'21) [36]	ResNet50	67.8	72.8	58.0	58.0	64.2	-	71.1	73.2	60.5	57.5	65.6	-
Baseline	ResNet50	62.5	69.4	58.9	55.9	61.7	72.0	63.2	70.5	60.1	57.6	62.9	74.4
SiGCN	ResNet50	65.1	70.1	65.2	60.8	65.3	77.5	68.9	72.6	66.8	65.8	68.5	78.3

		Results on COCO-20 ¹											
Methods	Backbone	1-shot					5-shot						
		Fold-0	Fold-1	Fold-2	Fold-3	Mean	FB-IoU	Fold-0	Fold-1	Fold-2	Fold-3	Mean	FB-IoU
FWB (ICCV'19) [17]	VGG16	18.4	16.7	19.6	25.4	20.0	-	20.9	19.2	21.9	28.4	22.6	-
PFENet (TPAMI'20) [24]	VGG16	33.4	36.0	34.1	32.8	34.1	60.0	35.9	40.7	38.1	36.1	37.7	61.6
SAGNN (CVPR'21) [27]	VGG16	35.0	40.5	37.6	36.0	37.3	61.2	37.2	45.2	40.4	40.0	40.7	63.1
RePRI (CVPR'21) [11]	ResNet50	31.2	38.1	33.3	33.0	34.0	-	38.5	46.2	40.0	43.6	42.1	-
SAGNN (CVPR'21) [27]	ResNet101	36.1	41.0	38.2	33.5	37.2	60.9	40.9	48.3	42.6	38.9	42.7	63.4
MMNet (ICCV'21) [26]	ResNet50	34.9	41.0	37.2	37.0	37.5	-	37.0	40.3	39.3	36.0	38.2	-
HSNet (ICCV'21) [15]	ResNet50	36.3	43.1	38.7	38.7	39.2	68.2	43.3	51.3	48.2	45.0	46.9	70.7
CyCTR (NIPS'21) [36]	ResNet50	38.9	43.0	39.6	39.8	40.3	-	41.1	48.9	45.2	47.0	45.6	-
Baseline	ResNet50	33.6	39.2	36.5	34.2	35.9	60.7	35.3	43.1	38.4	38.7	38.9	62.0
SiGCN	ResNet50	38.7	46.3	43.1	37.5	41.4	62.7	44.9	54.5	46.5	45.9	48.0	66.2

Ablations

		Components Analysis					FB-IoU
SiGR	IA	s^0	s^1	s^2	s^3	mean	
		62.5	69.4	58.9	55.9	61.7	72.0
	✓	62.0	70.0	58.5	59.4	62.7	73.5
✓		64.6	69.8	64.1	60.8	64.8	77.4
✓	✓	65.1	70.1	65.2	60.8	65.3	77.5

		GCN variants					FB-IoU
GCN Variants		s^0	s^1	s^2	s^3	mean	
baseline		62.0	70.0	58.5	59.4	62.7	73.5
GCN [7]		63.0	69.4	59.7	57.1	62.3	73.3
SiGCN-1		63.4	69.6	62.2	60.0	63.8	75.4
SiGCN-2		65.1	70.1	65.2	60.8	65.3	77.5

		Prototype number k					FB-IoU
k prototypes		s^0	s^1	s^2	s^3	mean	
1		64.8	69.7	63.5	59.0	64.3	75.9
3		64.1	70.2	64.3	59.5	64.5	76.2
5		65.1	70.1	65.2	60.8	65.3	77.5
7		63.7	69.8	63.8	60.2	64.4	75.5

Visualization



Acknowledgement: This work was partially funded by Elekta Oncology Systems AB and RVO public-private partnership grant (PPS2102).